JACS
JOURNAL OF THE AMERICAN CHEMICAL SOCIETY
Article
pubs.acs.org/JACS

Solvent Effects upon Guest Binding and Dynamics of a $Fe^{II}_4L_4$ Cage

Jeanne L. Bolliger, Tanya K. Ronson, Masahiro Ogawa, and Jonathan R. Nitschke*

Department of Chemistry, University of Cambridge, Lensfield Road, Cambridge CB2 1EW, United Kingdom

Supporting Information

ABSTRACT: Solvent-dependent host–guest chemistry and favoring of otherwise disfavored conformations of large guests has been achieved with an adaptive, self-assembled $Fe^{II}_4L_4$ coordination cage. Depending on the counterion, this face-capped tetrahedral capsule is soluble either in water or in acetonitrile and shows a solvent-dependent preference for encapsulation of certain classes of guest molecules. Quantitative binding studies were undertaken, revealing that both aromatic and aliphatic guests bind in water, whereas only aliphatic guests bind in acetonitrile. The flexibility of its subcomponent building blocks allows this cage to expand or contract upon guest binding, as studied by VT-NMR, thereby ensuring strong binding of both small and large guests. Upon encapsulation, large guest molecules can adopt conformations which are not thermodynamically favored in the free state. In addition, the chirotopic inner phase of the cage renders enantiotopic guest proton signals diastereotopic in specific cases.

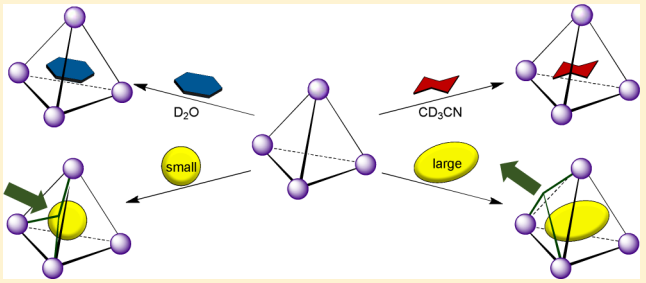

INTRODUCTION

Environment influences behavior, for molecules as much as for people. Recent years have seen increased interest in the use of the shielded inner phases of synthetic hosts to favor otherwise unfavorable conformations of guest species,[1] to shift equilibria,[2] and to stabilize reactive species.[3] Confinement inside hosts has been used to lower the symmetry of guests, thereby creating new means to control the outcomes of asymmetric reactions[2a,4] in the same way that biological systems make extensive use of tailored microenvironments to promote stereospecific reactions by destabilizing the ground state and stabilizing certain transition-state geometries.[5]

Self-assembly provides a straightforward means to prepare new host molecules. Small changes to the geometries of building blocks can lead to much larger changes in the structures and properties of the organic[6] or metal–organic cages[7] formed upon self-assembly. Modulation of the cavity environment can allow for selective binding in host materials.[8] As solvent effects can impact the guest-binding process in subtle and important ways,[9] control over host solubility through host framework charge and substituent effects provides further means to control guest binding strengths, selectivity, and dynamics.[10]

Here we present an in-depth study of the host–guest chemistry of a new $Fe^{II}_4L_4$ cage which self-assembles from a C_3-symmetric ligand, 2-formylpyridine, and an iron salt. Remarkably, this capsule is soluble both in acetonitrile and water, thereby allowing the investigation and comparison of its behavior and guest binding across different solvents.[11]

The flexibility of the side panels of our Fe_4L_4 cage allows the host to adapt to its guests, allowing strong binding of both small and large molecules. Due to the confined space inside this cage and the constraints imposed upon the bound species, certain guests are observed to adopt ground-state configurations which are unfavorable in their free states.

RESULTS AND DISCUSSION

Self-Assembly of Face-Capped $[Fe^{II}_4L_4]^{8+}$ Cages. Triamine **1** was synthesized in two steps from cyanuric chloride as shown in Scheme 1. The deep purple tetrahedral cage molecule **2** was then prepared as the triflate salt in deuterated acetonitrile from **1**, 2-formylpyridine, and iron(II) triflate in a 4:12:4 ratio via subcomponent self-assembly[12] and used as a stock solution for subsequent experiments. The $[Fe_4L_4]^{8+}$ structure of **2** was confirmed by ESI-MS (Figure S29) and by 2D NMR experiments (Figures S47–S53). VT NMR experiments indicated that the triflate counterion was not encapsulated in **2** (Figure S48); instead the cavity was occupied by the solvent acetonitrile which was in fast exchange on the ^{1}H NMR time scale (Figure S47) but in slow exchange on the DOSY time scale (Figure S50).

Cage **2** could be prepared in water-soluble form by employing iron(II) sulfate in a 1:1 mixture of acetonitrile/water in place of iron(II) triflate in pure acetonitrile. Removal of the solvent mixture and dissolution in neat D_2O led to the formation of [2-formylpyridine⊂**2**]$(SO_4)_4$ (Figures S55–S57): In water, **2** was always observed with a guest, and in the absence of added guest, 1/12 equiv of cage was observed to decompose in order to furnish 2-formylpyridine as a guest. Using 13 equiv of 2-formylpyridine (instead of 12) in the preparative self-assembly reaction, gave a clean solution of [2-formylpyridine⊂**2**]$(SO_4)_4$ containing no excess of triamine **1**,

Received: July 29, 2014
Published: September 16, 2014

   dx.doi.org/10.1021/ja5077102 | J. Am. Chem. Soc. 2014, 136, 14545–14553

Scheme 1. Synthesis of Triamine 1 and Subcomponent Self-Assembly of Cage 2

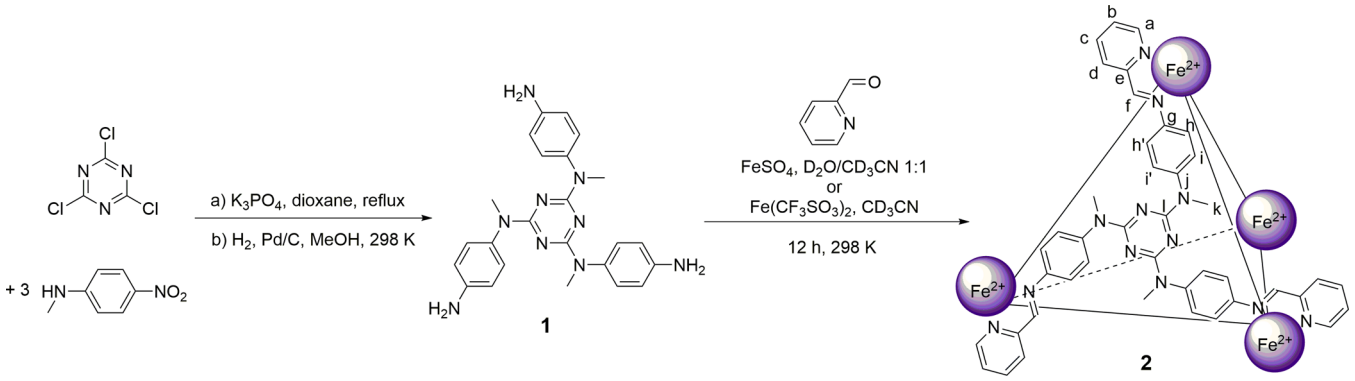

which could be used directly as a 1 mM stock solution for binding studies in D_2O.

X-ray quality crystals of $[\mathbf{2}](SO_4)_4$ were obtained through slow diffusion of THF into an aqueous solution (Figures 1 and S1). Capsule **2** crystallized in the cubic space group *I*23 with one-twelfth of the molecule in the asymmetric unit and crystallographic *T*-symmetry. The four octahedral iron(II) centers are bridged by four ligands, each of which caps a face of the tetrahedron. The ligands on the faces of **2** adopt a C_3-symmetric propeller-like configuration, in which the handedness of the propeller is the same as the handedness of the metal centers that they bridge, as has been observed for similar cage molecules.[7h] The cavity of **2** is almost completely enclosed due to the face-capped arrangement of ligands and the presence of methyl groups blocking the pores along the edges of the tetrahedron. The iron(II) centers are separated by 15.535(1) Å, and the volume of the central cavity was calculated to be 233 ± 2 Å^3 (Figure 1 and SI Section 1.3.2).[14] The amine nitrogen atoms of each ligand arm are planar, with C−N−C angles ranging from 114.3(5)° to 124.1(4)° (mean 120°) and are nearly coplanar with the central triazine ring (dihedral angle of 2°), while the phenyl and triazine rings form a dihedral angle of 42°.

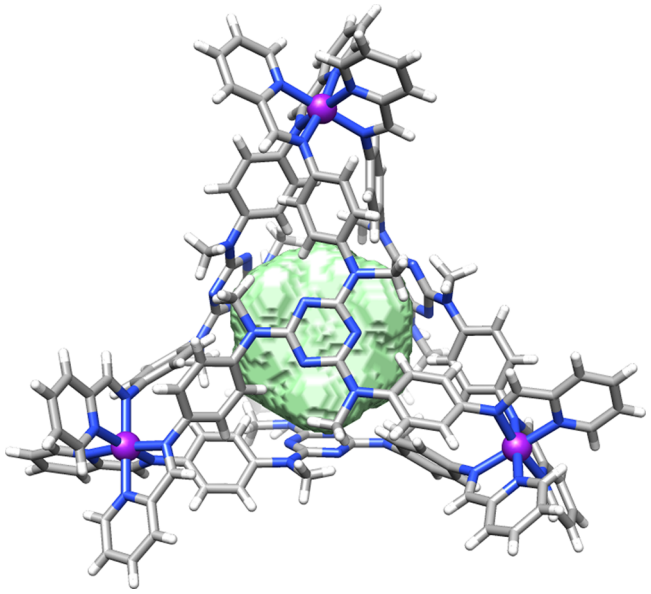

Figure 1. Crystal structure[13] of $[\mathbf{2}](SO_4)_4$ showing the cavity as calculated using VOIDOO.[14] The sulfate counterions are omitted for clarity.

Solvent-Dependent Host−Guest Chemistry. Binding studies were carried out at 298 K in deuterated water or acetonitrile using a 1.0 mM stock solution of [2-formylpyridine⊂**2**]$(SO_4)_4$ or $[\mathbf{2}](CF_3SO_3)_8$, respectively, to which an excess (~0.5 μL or 0.5 mg) of the guest was added.

Host **2** was observed to encapsulate a wide range of guests in water (Figure 2a), but only a subset of these molecules were found to bind in acetonitrile (Figure 2b). For example, we observed encapsulation of aromatic molecules to occur only in water, whereas aliphatic guests bound within **2** in both acetonitrile and water. This result is consistent with recent findings[10b] that aromatic guests experienced a greater driving force for encapsulation in a metal−organic host in water than in acetonitrile, whereas aliphatic guests did not. Polarizable aromatic guests thus appear to be better solvated in more-polarizable acetonitrile than in less-polarizable water. Also, cage **2** was observed to encapsulate larger guests in water than in acetonitrile, as observed in the case of (*R*)-limonene. We hypothesize that more water molecules order around a larger guest, generating a proportionally greater entropic driving force for binding than would be observed in acetonitrile.

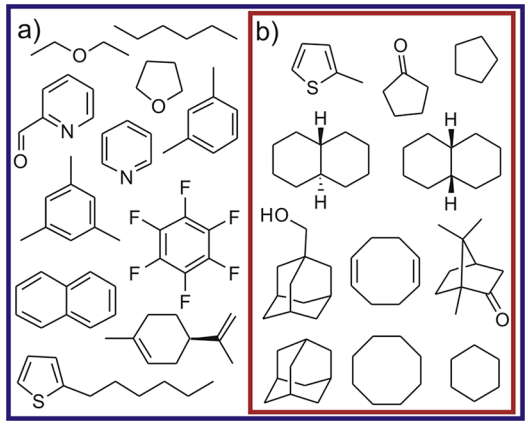

Figure 2. Guest molecules for **2**. In D_2O (a) all molecules were encapsulated in **2**, whereas in CD_3CN only a subset (b) was encapsulated.

1,3,5-Triethylbenzene, 8-phenyloctanol, tetraphenylmethane, and diphenylether were too large to bind in water; also the large, rigid aromatic guests biphenyl, phenanthrene, pyrene, fluorene, and anthracene were not observed to bind. Although

dx.doi.org/10.1021/ja5077102 | J. Am. Chem. Soc. 2014, 136, 14545−14553

the large anion triflimide ($(CF_3SO_2)_2N^-$) was encapsulated in acetonitrile, as evidenced by two sets of peaks in ^{1}H NMR and ^{19}F NMR spectra (Figures S161 and S162), the smaller anions $CF_3SO_3^-$, $CF_3CO_2^-$, BF_4^-, PF_6^-, GeF_6^{2-}, AsF_6^-, and SbF_6^- were not observed to bind to **2** in acetonitrile.[15] Also, glucose cyclododecane, 18-crown-6, 15-crown-5, and D-leucine were not observed to bind in either solvent.

Larger guests such as *cis*- and *trans*-decalin or 2-hexylthiophene required up to 2 weeks for equilibration at room temperature, whereas smaller guests such as THF, cyclopentane, or hexafluorobenzene were observed to be taken up by **2** in <1 h. The smallest prospective guests, dichloromethane and acetonitrile, showed evidence of rapid exchange between the bound and unbound states on the NMR time scale. Dichloromethane showed evidence of binding in D_2O by NOESY (Figure S164), while encapsulated acetonitrile was observed in CD_3CN by DOSY (Figure S50). In both cases only one set of host and guest peaks was observed in the ^{1}H NMR spectrum.

Following the uptake of slow-exchanging guests, a second set of peaks appeared in the ^{1}H NMR spectrum, assigned to the host–guest complex [guest⊂**2**]. For soluble guests, two sets of guest peaks were observed, which were assigned to the encapsulated and free guests. Exchange between free and encapsulated guests was slow on both ^{1}H NMR and DOSY time scales. Encapsulation was further confirmed by both DOSY NMR, where the encapsulated guest and host were observed to diffuse at the same rate, and by NOESY, where cross peaks between guest and cage protons consistent with encapsulation were observed.

ESI mass spectra also supported the formation of host guest complexes in acetonitrile (Figures S30–S37), with host–guest complexes being detected intact in many cases. Smaller guests were lost more easily upon ionization, such as with [cyclopentanone⊂**2**] (Figure S37). In cases where incomplete host–guest complex formation was observed, as with [*cis*-decalin⊂**2**]-$(CF_3SO_3)_8$, we also observed the CD_3CN complex of **2** (Figure S33) in the ESI spectra.

The binding constants listed in Table 1 were determined by ^{1}H integration, following addition of the guest to a stock solution of host, prepared as described above. In water they thus represent the guest's binding affinity relative to the 2-formylpyridine guest present in the [2-formylpyridine⊂**2**]-$(SO_4)_4$ stock solution employed, and in acetonitrile solution, guest affinity relative to acetonitrile. Each experiment was carried out three or four times at varying host:guest ratios; the average binding constants with standard deviations are given in logarithmic form. For those guests that were not sufficiently water-soluble to be observed by ^{1}H NMR, the percentage encapsulation following addition of excess guest (4–8 equiv, 0.5 mg of solids or 0.5 μL of liquids) is given.

The binding affinities were observed to depend on the size, shape, and polarity of the guests. Spherical molecules such as adamantane appeared to bind more strongly than linear or flat molecules, which we infer to result from a good size and shape fit between guest and cavity (Figure 1).

Guest-Dependent Host Dynamics. As observed in the molecular models (Figures S2–S25), the amines linking the central triazine panels to the phenylene groups are known to rehybridize readily from a flat sp^2 toward a pyramidal sp^3 configuration.[16] Since the faces of the tetrahedral cage are not rigid, **2** can either contract (Figure 3a) or expand (Figure 3b) its cavity and thereby adapt itself to the size of the encapsulated guest. Models suggest that when binding a small guest, the phenylene rings of **2** gear together tightly (Figure 3c), resulting

Table 1. Binding Constants for 2 in D_2O[a] and CD_3CN[b]

guest	log(K_a) relative to 2-formylpyridine[a,c] or [G⊂H]/[H]$_0$[d] in D_2O	log(K_a) relative to acetonitrile in CD_3CN[b,e,f]
diethyl ether	−0.16 (±0.07)	no binding
2-formylpyridine	0.00 (defined)[a,c]	no binding
pyridine	0.03 (±0.06)[a,c]	no binding
tetrahydrofuran	0.25 (±0.04)[a,c]	no binding
mesitylene	0.59 (±0.01)[a,c]	no binding
cyclopentanone	0.82 (±0.05)[a,c]	1.74 (±0.04)[e]
m-xylene	1.06 (±0.05)[a,c]	no binding
camphor	1.18 (±0.11)[a,c]	3.55 (±0.04)[f]
hexafluorobenzene	1.21 (±0.03)[a,c]	no binding
cyclopentane	1.27 (±0.03)[a,c]	2.71 (±0.02)[e]
1-adamantylmethanol	1.48 (±0.05)[a,c]	3.15 (±0.06)[e]
		3.11 (±0.04))[f]
2-methylthiophene	2.42 (±0.02)[a,c]	1.39 (±0.08)[e]
cyclohexane	2.78 (±0.05)[a,c]	3.85 (±0.04)[f]
		4.09 (±0.06)[e]
1,5-cyclooctadiene	3.11 (±0.05)[a,c]	3.58 (±0.08)[f]
2-hexylthiophene	69.1 (±3.9)%[d]	no binding
trans-decalin	94.9 (±1.4)%[d]	1.22 (±0.10)[e]
cis-decalin	100%[d]	2.54 (±0.03)[e]
cyclooctane	100%[d]	3.91 (±0.04)[f]
adamantane	100%[d]	4.32 (±0.04)[f]
R-limonene	100%[d]	traces
naphthalene	100%[d]	no binding

[a]Calculated relative to 2-formylpyridine. [b]Calculated relative to acetonitrile. [c]Slightly water-soluble guests, competition experiments with THF and 1,5-cyclooctadiene. [d]Guests that are insoluble in water, proportion of host–guest complex relative to the total amount of guest added. [e]Direct binding constants. [f]Binding constants derived from competition experiments with cyclopentane or 1,5-cyclooctadiene.

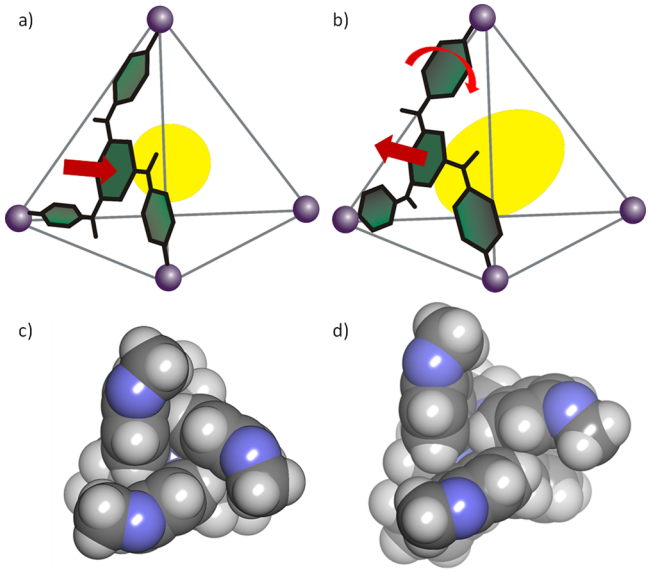

Figure 3. Schematic diagrams showing the adaptation of **2** to (a) a small and (b) a large guest. (c and d) Corners of molecular models viewed from the inside toward a Fe^{II} center showing the inferred (c) gearing together of the phenylene groups in the case of the small guest adamantane and (d) pushing apart of the phenylenes for the larger guest 1-adamantylmethanol.

dx.doi.org/10.1021/ja5077102 | J. Am. Chem. Soc. 2014, 136, 14545–14553

in blocked rotation, whereas binding a large guest prises the phenylene rings apart (Figure 3d), allowing them to spin more freely.

Rebek's 55% optimal-occupancy "rule"[18] has recently been validated in the case of a rigid metal–organic host–guest system, where the strongest binding was found for a guest occupying ca. 55% of the cavity volume.[18,19] No correlation was found, however, between the binding affinities of **2** for the guests and the degree of host cavity occupation (Table S1 and Figure S28). The void volume of **2** in its compressed state was determined to be 233 ± 2 Å^3 from the crystal structure (Figure 1), but we infer the cavity volume of **2** to vary considerably based upon guest size: volumes of **2** derived from the molecular models of host–guest complexes (Figures S2–S25) ranged from 261 ± 2 Å^3 for [pyridine⊂**2**] to 347 ± 1 Å^3 for [2-hexylthiphene⊂**2**]. The flexibility of **2** thus renders the concept of cavity volume less useful than it might be in more rigid systems.[19]

^{1}H NMR spectra of [adamantane⊂**2**] and [1-adamantylmethanol⊂**2**] are presented in Figure 4 as examples of host–guest complexes with smaller and larger guests, respectively.

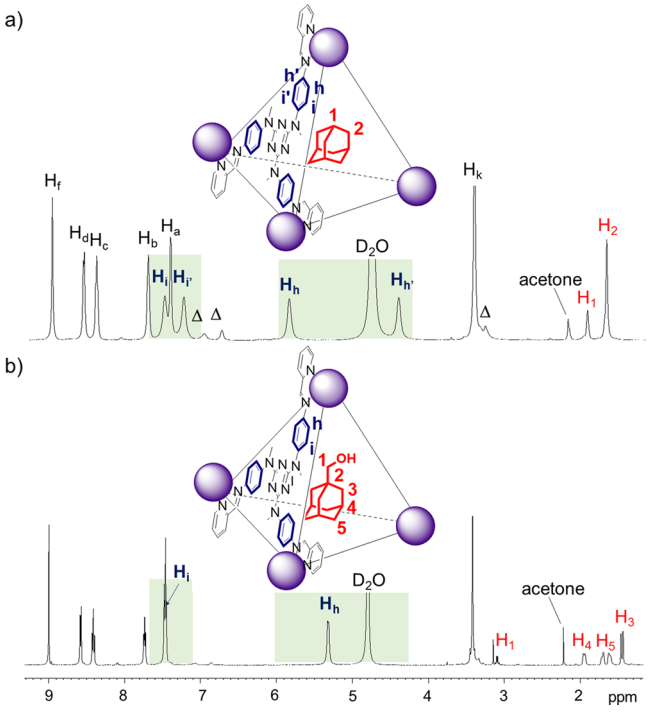

Figure 4. ^{1}H NMR spectra at 298 K of (a) [adamantane⊂**2**] in D_2O and (b) [1-adamantylmethanol⊂**2**] in D_2O. The peaks marked with Δ correspond to excess free triamine **1**.

Figure 5 provides a plot of the largest guest dimension (*d*) against the energetic barrier to rotation of the phenylene groups ($\Delta G^{\ddagger}$) as determined by measuring the temperature at which the ^{1}H NMR signals of H_h and H_i coalesce with H_h' and H_i'. A linear relationship was observed between these two parameters, such that $\Delta G^{\ddagger} = -3.30d + 74.7$. The longest guest dimension *d* (including van der Waals radii) was determined with Accelrys Discovery Studio[17] (SI Section 2.2) using MM2-optimized molecular models of the corresponding guests as a basis. This relationship is consistent with our inference that the encapsulation of larger guests results in a bowing out of the cage faces, allowing the phenylene rings to spin more freely. No

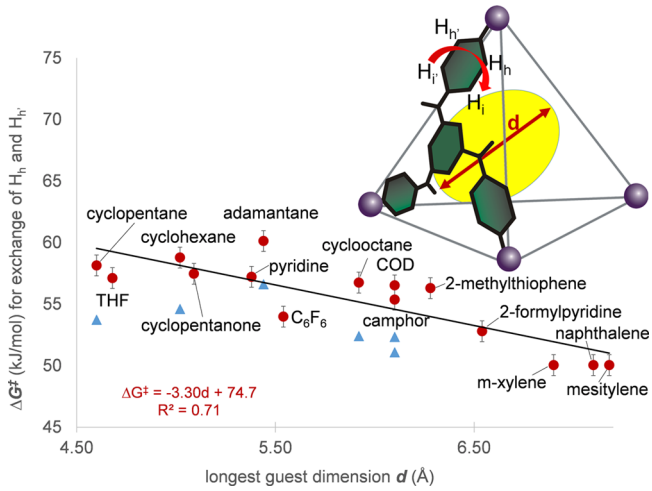

Figure 5. Linear relationship between the free activation energy for the rotation of the phenylene rings and the longest guest dimension. Red circles, in D_2O; blue triangles, in CD_3CN.

correlation was observed between $\Delta G^{\ddagger}$ and volume (Figure S27a) or partition coefficient (Figure S27b).

The guest-dependent dynamics of the phenylene groups of **2** were similar in acetonitrile (Figure 5, blue triangles) to what was observed in water (Figure 5, red circles), although not enough data were available to allow a correlation between $\Delta G^{\ddagger}$

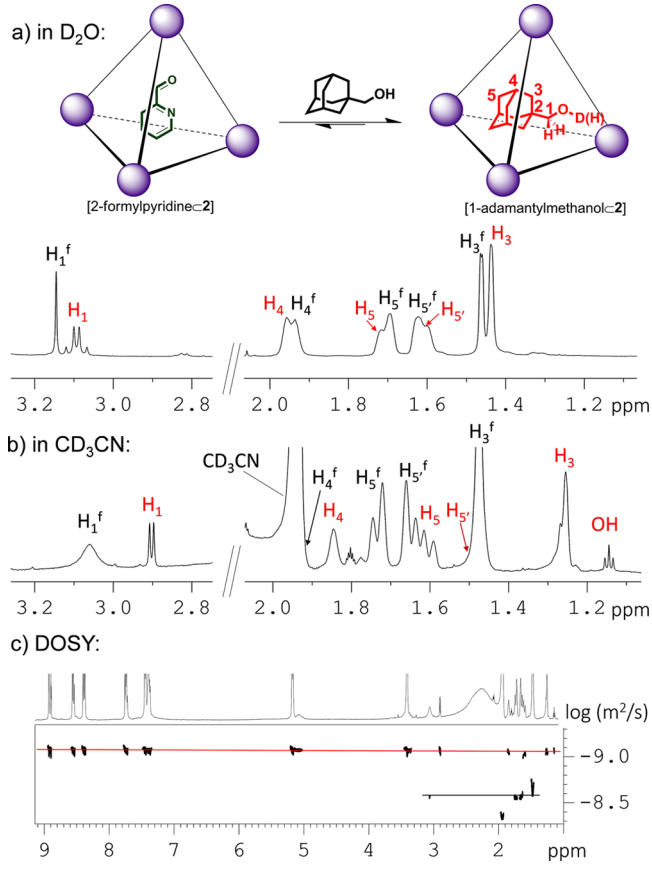

Figure 6. ^{1}H NMR spectra of [1-adamantylmethanol⊂**2**] in (a) D_2O and (b) CD_3CN. (c) DOSY in CD_3CN; signals labeled with superscript "f" correspond to the free guest, while others correspond to bound guest.

dx.doi.org/10.1021/ja5077102 | J. Am. Chem. Soc. 2014, 136, 14545–14553

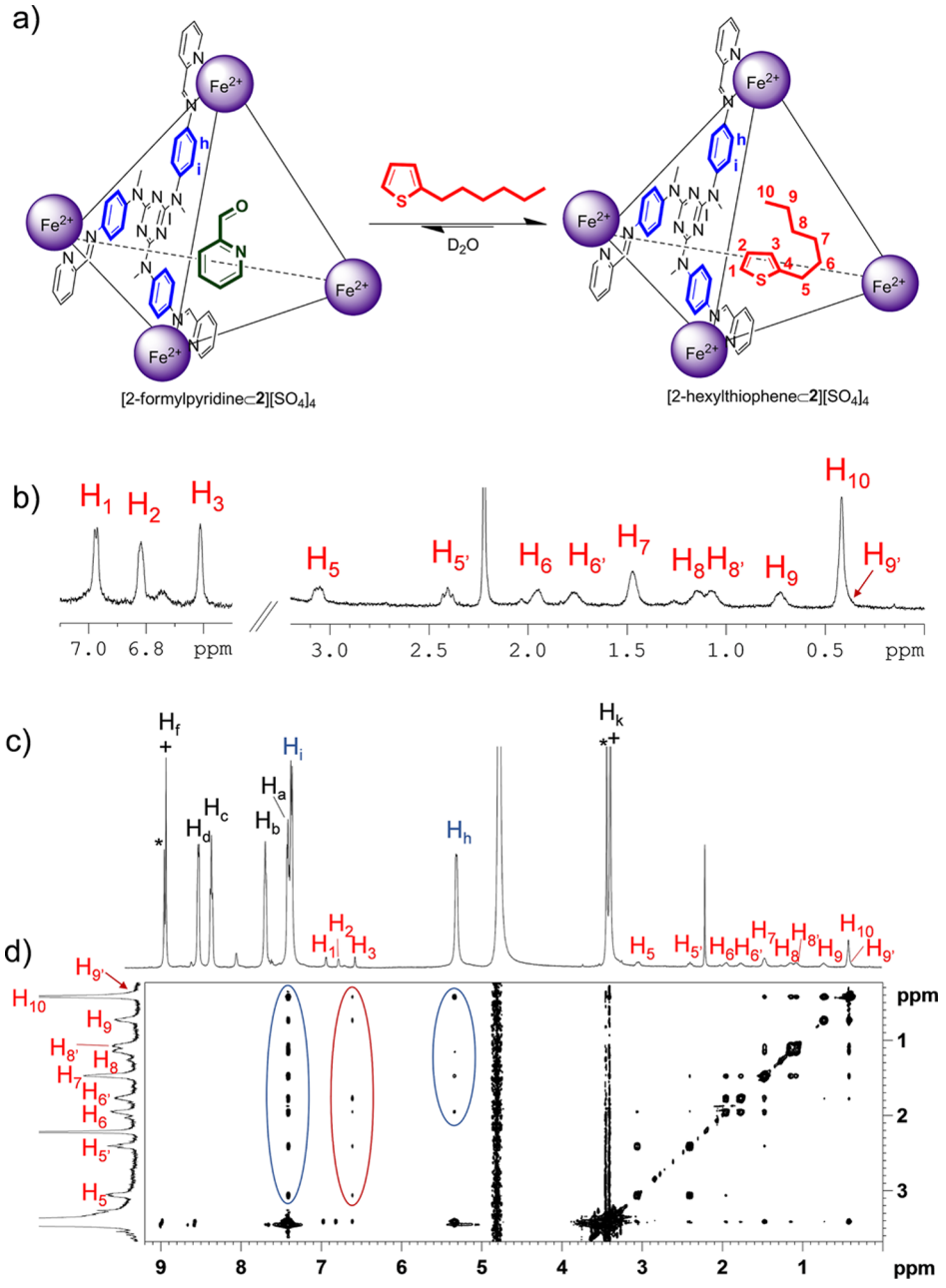

Figure 7. [2-hexylthiophene⊂**2**]. (a) Encapsulation in D_2O; (b) expansion of the guest peaks of the ^1H NMR spectrum of 2-hexylthiophene in **2**; (c) full ^1H NMR spectrum with "+" denoting [2-hexylthiophene⊂**2**] and "*" corresponding to [2-formylpyridine⊂**2**]; (d) NOESY spectrum with relevant host-guest crosspeaks circled in blue and guest-guest peaks circled in red.

and *d* to be inferred in this solvent. We note, however, that $\Delta G^{\ddagger}$ for a given guest was uniformly observed to be greater by a factor of 1.08 (±0.008) in water than in acetonitrile. This differential can be considered as a manifestation of the greater magnitude of solvophobic effects in water than in acetonitrile,[10b] expressed as a greater force pushing the walls of the cage inward.

Proton Exchange Modulation through Encapsulation. The inner phase of **2** effectively isolates guests from the solvent environment. A novel manifestation of this effect was observed following the binding in water and acetonitrile of 1-adamatylmethanol (Figure 6). When free in aqueous solution, its hydroxyl proton was not visible in the ^1H NMR spectrum due to rapid proton exchange with the solvent, and the exocyclic methylene group appears as a singlet. Following encapsulation, however, this methylene group gave rise to a signal corresponding to two overlapping 1:1:1 triplets, consistent with coupling to the OD deuterium (Figure 6a). We infer that the chirotopic inner phase of **2** renders these ordinarily enantiotopic protons diastereotopic, resulting in the observed splitting.

In acetonitrile, the hydroxyl protons of free 1-adamantylmethanol were not observed by NMR; we infer that they are observed together with the signal from the H_2O formed during the condensation of the ligands of **2**, in fast exchange. Encapsulation prevents this exchange, however, causing the hydroxyl group of encapsulated 1-adamantylmethanol to be observed as a triplet due to coupling with the exocyclic CH_2 group, which is observed as a doublet (Figure 6b). These enantiotopic methylene protons thus do not experience the

dx.doi.org/10.1021/ja5077102 | J. Am. Chem. Soc. 2014, 136, 14545−14553

chirotopic environment of the cage's interior in acetonitrile, in contrast with their diastereotopic behavior in water.

The greater sense of chirotopicity experienced by the guest in water may be a consequence of the stronger solvophobic interactions experienced by the host in this solvent, as compared to acetonitrile.[20] As discussed above, the faces of host **2** are compressed inward in water, as manifested by a higher barrier to rotation of its pressed-together phenylene groups in water than in acetonitrile (Figures 5 and S26). The external pressure imposed by the hydrophobic effect may thus lead to a more intimate contact between guest and host, causing the guest to experience a chirotopic host environment in water but not in acetonitrile.[21] NMR of the exocyclic methylene group of 1-adamantylmethanol, or a structurally related molecule, may prove a useful probe for measuring the "degree of chirotopicity" in its local environment, which may have relevance in the context of stereoseletive transformations in such environments.

Larger Guests Reorganize to Fit Within 2. In order to fit into the confined cavity of aqueous host **2**, 2-hexylthiophene adopts a coiled conformation that is thermodynamically unfavorable in its free state (Figure 7a). As with 1-adamatylmethanol, most of the CH_2 protons of 2-hexylthiophene experience a diastereotopic environment and are observed as peaks which integrate to a single proton (Figure 7b). The phenylene cage peaks for [2-hexylthiophene⊂**2**] again rotate quickly on the NMR time scale, consistent with the relatively large size of this guest. Reinforcing the status of 2-hexylthiophene as the largest molecule that can undergo encapsulation within **2**, we in all cases observed a 7:3 mixture of [2-hexylthiophene⊂**2**] and [2-formylpyridine⊂**2**] (Figure 7c). As has been reported by Rebek's group,[22] we propose a folded conformation of the hexyl chain in [2-hexylthiophene⊂**2**], as shown in Figure 7a. NOE cross peaks between H_1 of the thiophene unit and the CH_3 group of the hexyl chain confirm this inference, and the other NOE cross peaks, both cage-guest and intraguest, further support our proposed guest conformation (Figure 7d).

A molecular model of [2-hexylthiophene⊂**2**] (Figure 8) from molecular mechanics calculations carried out with ArgusLabs[23] using the universal force field (UFF) is in agreement with the structure derived from NMR measurements. In addition, it shows that due to the conformational change of the guest in [2-hexylthiophene⊂**2**], it adopts a more spherical shape and can be encapsulated without distortion of host **2**. Restricted motions, such as freezing out of ring flipping or allowing the adoption of only one conformation among several, have been observed upon encapsulation to result in a lower apparent symmetry of the encapsulated guest.[24]

Both isomers of decalin were found to be competent guests for **2** in D_2O, with *cis*-decalin binding more than five times more strongly than the *trans*-diastereomer (Figure 9a–c). Whereas [*cis*-decalin⊂**2**] displayed only very broad and overlapping guest ^1H signals, which we could not assign to specific conformers of the cyclohexane rings, the [*trans*-decalin⊂**2**] complex showed nine sets of peaks in the ^1H NMR spectrum for the encapsulated guest, which integrate to two protons each, indicating that the guest had lost a C_2 symmetry axis upon encapsulation.[25] Since the cage framework still displayed tetrahedral symmetry in the [*trans*-decalin⊂**2**] complex, we infer that the guest is still tumbling inside the cage and that this loss of guest symmetry is the result of the adoption of a boat–boat (or twist–boat–twist–boat) conformation. The desymmetrization of the guest from C_{2h} to C_i symmetry is also supported by the observation of five distinct carbon signals, of which two overlap, in the corresponding HSQC spectrum. We infer that whereas *cis*-decalin fits better into the cage, *trans*-decalin is slightly too large in its chair–chair form. By adopting a boat–boat conformation (or twist–boat), encapsulation becomes possible.

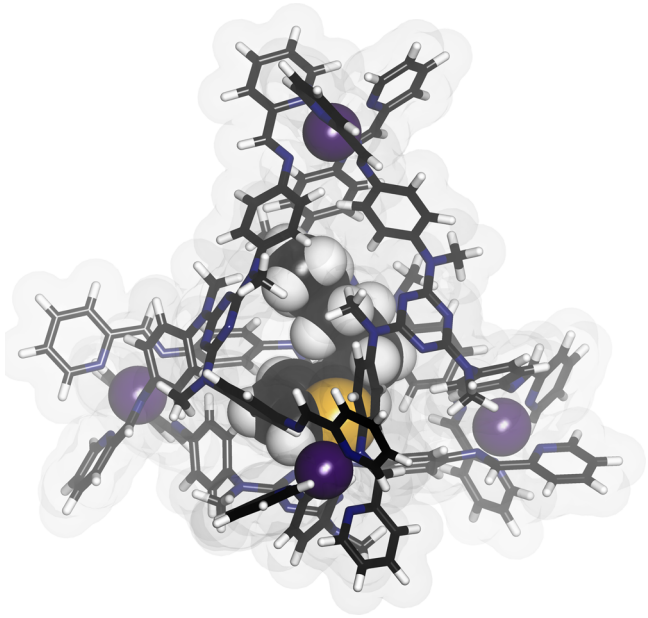

Figure 8. Molecular model of [2-hexylthiophene⊂**2**] from molecular mechanics calculations with ArgusLabs using the UFF.[23]

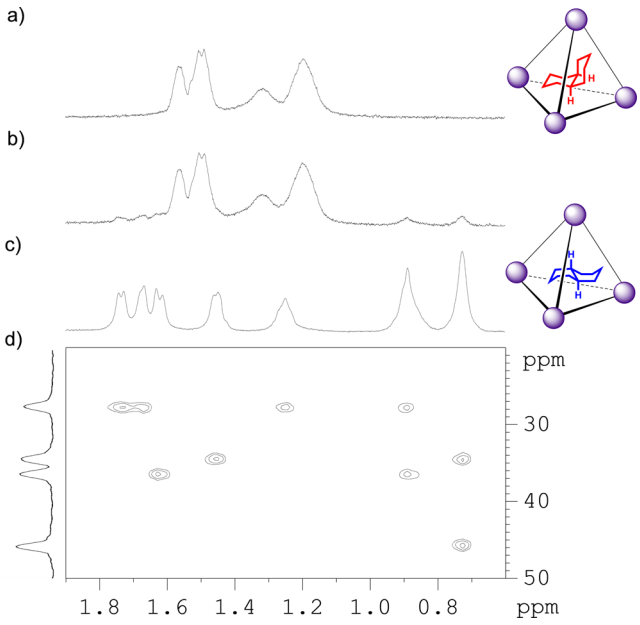

Figure 9. ^1H NMR spectra of (a) [*cis*-decalin⊂**2**]; (b) [*cis*-decalin⊂**2**] binding in preference to [*trans*-decalin⊂**2**]; (c) [*trans*-decalin⊂**2**]; and (d) HSQC spectrum of [*trans*-decalin⊂**2**].

Chiral Guests. Cage **2** consists in solution as a racemic mixture of homochiral cages, in which all the iron centers possess either Δ or Λ stereochemistry.[26] In similar fashion to what was observed when chiral guests were bound within a $Fe^{II}_4L_6$ cage,[27] we observed splitting of both host and guest peaks in the ^1H NMR and ^{13}C NMR spectra upon the addition

dx.doi.org/10.1021/ja5077102 | J. Am. Chem. Soc. 2014, 136, 14545–14553

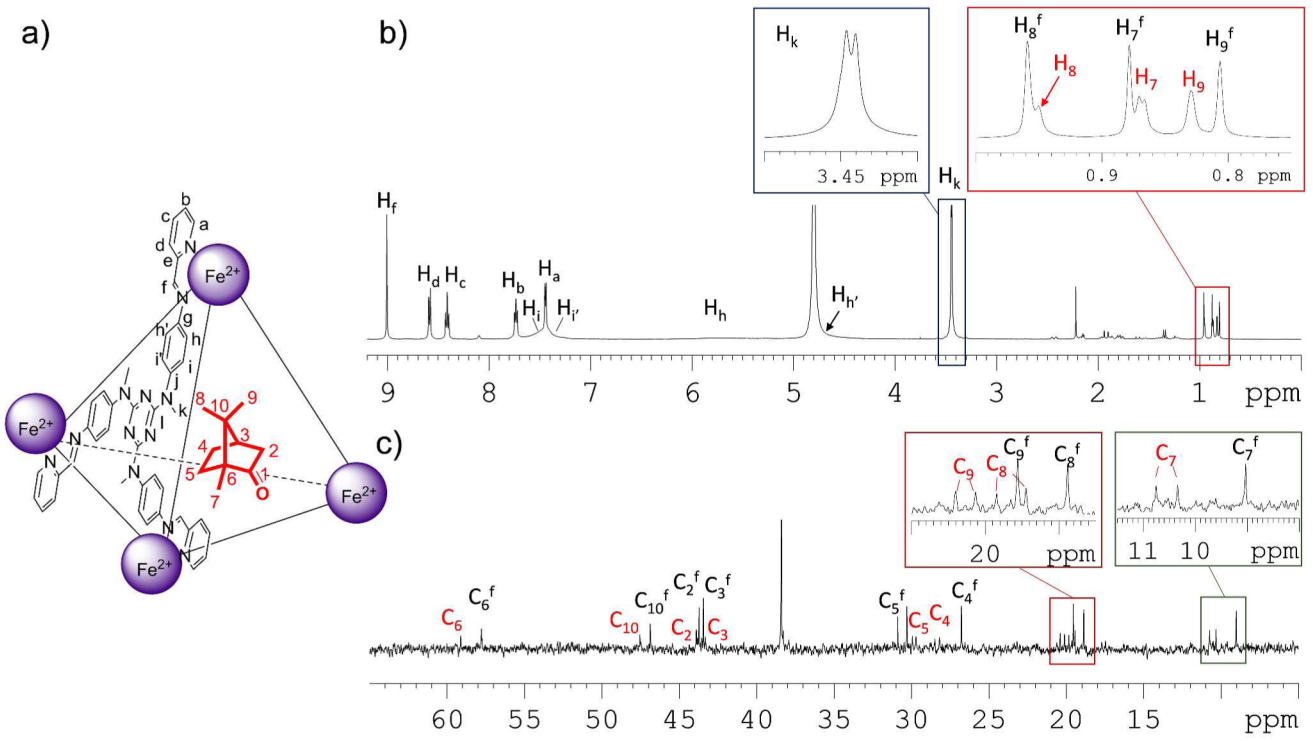

Figure 10. (a) Labeled diagram showing the encapsulation of camphor within **2**. (b) ^{1}H NMR in D_2O and (c) ^{13}C NMR spectra in D_2O of the host–guest complex, showing splitting due to the presence of both cage enantiomers. Signals labeled with superscript "f" correspond to the free guest, while others correspond to bound guest.

of an excess of a chiral guest such as (*1R*)-camphor both in water and in acetonitrile (Figure 10b,c). The presence of these peaks is consistent with the presence of diastereomeric host–guest complexes [(*1R*)-camphor⊂ΔΔΔΔ-**2**] and [(*1R*)-camphor⊂ΛΛΛΛ-**2**], in a 1:1 ratio. The same ratio was also observed when adding a substoichiometric amount (0.33 equiv) of (*1R*)-camphor; this ratio was not observed to change after 14 days, suggesting that no discriminatory binding was taking place. Similar NMR splitting behavior without diastereoselective binding was observed with (*R*)-limonene in water; this guest was not observed to bind in acetonitrile, possibly due to a poor size fit.

CONCLUSIONS

Cage **2** thus binds a wide variety of guests in water and a subset of these in acetonitrile. The behavior of some of these guests is altered in subtle and interesting ways, and the cage walls flex in such a way as to effectively isolate guests from the solvent environment. The combination of straightforward preparation, robustness, usefulness in different solvents and a cavity volume large enough to encapsulate chemically complex guests renders **2** of great practical value in host–guest studies. We anticipate that **2** may become useful in altering the reactivities of guests, in addition to their conformations, as well as shuttling guest species between phases.

EXPERIMENTAL SECTION

General. Most reagents and solvents were purchased and used as supplied. D_2O and CD_3CN for cage stock solutions were carefully degassed by 3–4 freeze–pump–thaw cycles prior to use. ^{1}H NMR spectra were all recorded at 500.13 MHz on either a Bruker AVC-500 spectrometer with a TCI probe, a Bruker AVC-500 spectrometer with a ATM BB probe, or a Bruker AVC-500 spectrometer with a DUAL 500 ^{1}H/^{13}C cryoprobe. ^{13}C{^{1}H} NMR spectra were recorded at 125.76 MHz on a Bruker AVC-500 spectrometer with a DUAL 500 ^{1}H/^{13}C cryoprobe. ^{19}F NMR spectra were recorded on a Bruker AVC-400 spectrometer with a QNP probe. Chemical shifts (δ_H) are expressed in parts per million (ppm) and reported relative to the resonance of the residual protons of CD_2Cl_2 (δ_H = 5.32 ppm) and CD_3CN (δ_H = 1.94 ppm) or relative to the internal standard acetone (δ_H = 2.22 ppm) for samples in D_2O. ^{19}F chemical shifts (δ) are reported relative to hexafluorobenzene at 163.9 ppm. Coupling constants (J) are given in Hz. All measurements were carried out at 298 K unless stated differently. Abbreviations used in the description of NMR data are as follows: bs, broad singlet; s, singlet; d, duplet; t, triplet; m, multiplet. Elemental analyses were performed on an Exeter Analytical CE-440 Analyzer at the University of Cambridge, Department of Chemistry, U.K. Low-resolution electrospray ionization mass spectra (ESI-MS) were obtained on a Micromass Quattro LC, infused from a Harvard Syringe Pump at a rate of 10 μL per minute.

Compound 1. *N2,N4,N6-Trimethyl-N2,N4,N6-tris(4-nitrophenyl)-1,3,5-triazine-2,4,6-triamine.* In a round bottomed flask, 400 mL of dioxane was added to 1.844 g (10 mmol) cyanuric chloride, 5.018 g (33 mmol) *N*-methyl-4-nitroaniline, and 14.84 g (70 mmol) K_3PO_4. The reaction mixture was stirred under reflux for 96 h and then cooled to room temperature. The solid product was filtered off, washed with water (3 × 100 mL), methanol (3 × 100 mL), and diethyl ether (3 × 100 mL), and dried under vacuum to give the desired product in 76% (4.039 g, 7.6 mmol) yield. Elemental analysis (%) calcd for $C_{24}H_{21}N_9O_6$: C, 54.24; H, 3.98; N, 23.72; found: C, 54.00; H, 3.96; N, 23.50. ^{1}H NMR (500 MHz, CD_2Cl_2, 298 K): δ = 8.14 (d, ^{3}J = 8.9 Hz, 6H), 7.51 (d, ^{3}J = 8.9 Hz, 6H), 3.47 (s, 9H); ^{13}C{^{1}H} NMR (125 MHz, CD_2Cl_2, 298 K): δ = 165.5, 150.6, 144.5, 126.3, 124.0, 37.3.

N2,N4,N6-Tris(4-aminophenyl)-N2,N4,N6-trimethyl-1,3,5-triazine-2,4,6-triamine (1). In a round bottomed flask with 2.004 g (3.84 mmol) of N2,N4,N6-trimethyl-N2,N4,N6-tris(4-nitrophenyl)-1,3,5-triazine-2,4,6-triamine, 10% Pd/C (500 mg, 10 wt %) and 300 mL of MeOH were first placed under nitrogen then H_2 (1 atm, balloon). The reaction mixture was stirred for 24 h at room temperature and then filtered through Celite giving a colorless solution. The solvent

dx.doi.org/10.1021/ja5077102 | J. Am. Chem. Soc. 2014, 136, 14545–14553

was evaporated, and the pure product was obtained as a colorless powder in 93% (1.58 g) yield. Elemental analysis (%) calcd for $C_{24}H_{27}N_9{\cdot}0.25H_2O$: C, 64.63; H, 6.21; N, 28.26; found: C, 64.67; H, 6.18; N, 28.29. ^{1}H NMR (500 MHz, CD_2Cl_2, 298 K): δ = 7.03 (d, ^3J = 8.6 Hz, 6H), 6.58 (d, ^3J = 8.6 Hz, 6H), 3.63 (bs, 6H), 3.28 (s, 9H); ^{13}C{^{1}H} NMR (125 MHz, CD_2Cl_2, 298 K): δ = 165.9, 144.2, 136.6, 127.6, 114.8, 37.5.

[2](CF$_3$SO$_3$)$_8$ (1 mM solution in CD$_3$CN). In a glovebox, $Fe(CF_3SO_3)_2$ (19.2 mg, 0.054 mmol), triamine **1** (24.8 mg, 0.056 mmol) and 2-formylpyridine (15.5 μL, 0.163 mmol) were stirred for 12 h in a vial containing 13.5 mL of CH_3CN. The resulting purple 1 mM solution of $[\mathbf{2}](CF_3SO_3)_8$ was used directly without purification for host–guest studies. ^{1}H NMR (500 MHz, CD_3CN, 298 K, referenced to acetonitrile): δ 9.00 (s, 12H, H_f), 8.54 (d, ^3J = 7.6 Hz, 12H, H_d), 8.38 (unresolved dd, 12H, H_c), 7.73 (unresolved dd, 12H, H_b), 7.41–7.36 (m, 36H, H_a, H_i = $H_{i'}$), 5.08 (bs, 24H, H_h = $H_{h'}$), 3.41 (s, 36H, H_k); ^{13}C{^{1}H} NMR (125 MHz, CD_3CN, 298 K, referenced to acetonitrile): δ = 176.9 (C_f), 166.6 (C_l), 160.4 (C_e), 157.8 (C_a), 147.5 (C_g), 146.3 (C_j), 141.7 (C_c), 133.0 (C_d), 131.6 (C_b), 127.1 (C_i = $C_{i'}$), 123.0 (C_h = $C_{h'}$), 39.1 (C_k); ^{19}F{^{1}H} NMR (363 MHz, D_2O, 300 K): δ = −76.3 (bs, free OTf−); ESI-MS: m/z: $\{[\mathbf{2}] + CF_3SO_3\}^{7+}$ = 458.2, $\{[\mathbf{2}] + 2CF_3SO_3\}^{6+}$ = 559.4, $\{[\mathbf{2}] + 3CF_3SO_3\}^{5+}$ = 701.2, $\{[\mathbf{2}] + 4CF_3SO_3\}^{4+}$ = 913.3, $\{[\mathbf{2}] + 5CF_3SO_3\}^{3+}$ = 1267.9.

[2](SO$_4$)$_4$. $FeSO_4{\cdot}7H_2O$ (139.7 mg, 0.502 mmol), triamine (**1**) (221.5 mg, 0.501 mmol), and 2-formylpyridine (143 μL, 1.503 mmol) were added to a 250 mL round-bottomed flask with a nitrogen tap containing acetonitrile (30 mL) and distilled water (30 mL). The reaction mixture was carefully degassed by three freeze–pump–thaw cycles and then left to stir for 12 h at room temperature to give $[\mathbf{2}](SO_4)_4$. ^{1}H NMR (500 MHz, D_2O/CD_3CN 1:1, 298 K, referenced to acetonitrile): δ = 8.82 (s, 12H, H_f), 8.48 (d, ^3J = 7.5 Hz, 12H, H_d), 8.35 (unresolved dd, 12H, H_c), 7.70 (unresolved dd, 12H, H_b), 7.35–7.34 (m, 36H, H_a and H_i = H_i'), 5.02 (bs, 24H, H_h = $H_{h'}$), 3.33 (s, 36H, H_k); ^{13}C{^{1}H} NMR (125 MHz, D_2O/CD_3CN 1:1, 298 K, referenced to acetonitrile): δ = 175.5 (C_f), 165.3 (C_l), 159.0 (C_e), 156.6 (C_a), 146.5 (C_g), 145.0 (C_j), 140.7 (C_c), 131.8 (C_d), 130.6 (C_b), 126.0 (C_i = $C_{i'}$), 121.9 (C_h = $C_{h'}$), 38.1 (C_k).

[2-formylpyridine⊂2](SO$_4$)$_4$. Removal of the solvent mixture from $[\mathbf{2}](SO_4)_4$ and redissolving in D_2O resulted in the formation of [2-formylpyridine⊂**2**]$(SO_4)_4$ which was used directly as a 1 mM solution for binding studies in D_2O. ^{1}H NMR (500 MHz, D2O, 298 K, referenced to acetone): δ = 9.90 (s, 1H, encapsulated 2-formylpyridine, H_1), 9.00 (s, 12H, H_f), 8.66 (s, 1H, encapsulated 2-formylpyridine, H_6), 8.58 (d, ^3J = 7.6 Hz, 12H, H_d), 8.41 (t, ^3J = 7.7 Hz,, 12H, H_c), 7.73 (t, ^3J = 6.6 Hz, 12H, H_b), 7.70–7.60 (m, 2H, encapsulated 2-formylpyridine, H_3 and H_4), 7.44 (d, ^3J = 5.1 Hz, 12H, H_a), 7.41 (bs, 24H, H_i = $H_{i'}$ and encapsulated 2-formylpyridine, H_5), 5.26 (bs, 24H, H_h = $H_{h'}$), 3.45 (s, 36H, H_k); ^{13}C{^{1}H} NMR (125 MHz, D2O, 298 K, referenced to acetone): δ = 193.0 (encapsulated 2-formylpyridine, C_1), 175.4 (C_f), 164.7 (C_l), 158.7 (C_e), 156.3 (C_a), 153.9 (encapsulated 2-formylpyridine, C_2), 150.5 (encapsulated 2-formylpyridine, C_6), 146.8 (C_g), 144.2 (C_j), 140.3 (C_c), 136.3 (encapsulated 2-formylpyridine, C_4), 131.5 (C_d), 130.0 (C_b), 127.3 (encapsulated 2-formylpyridine, C_5), 125.8 (broad, C_i = $C_{i'}$), 121.7 (broad, C_h = $C_{h'}$), 119.0 (encapsulated 2-formylpyridine, C_3), 38.2 (C_k).

Host–Guest Studies with One Guest. In a glovebox, a NMR tube was charged with 0.5–0.7 mL of the 1.0 mM stock solution of [2-formylpyridine⊂**2**]$(SO_4)_4$ or $[\mathbf{2}](CF_3SO_3)_8$, respectively, to which an excess (~0.5 μL or 0.5 mg) of the guest was added. After closing the NMR tube, the reaction mixture was shaken carefully for about 15 s and then stored at 298 K until the host–guest experiment was equilibrated as shown by ^{1}H NMR spectra recorded periodically. Generally equilibration times were short (<1 h) for small guests such as THF, cyclopentane, or hexafluorobenzene, whereas large guests such as *cis*- or *trans*-decalin required up to 2 weeks for equilibration at room temperature. The NMR tubes were stored at 298 K until all NMR experiments were completed. VT NMR spectra were recorded last.

Competition Experiments. *In D$_2$O.* In a glovebox, a NMR tube was charged with 0.5–0.7 mL of the 1.0 mM stock solution of [2-formylpyridine⊂**2**]$(SO_4)_4$ and about 0.5 μL of THF or 1,5-cyclooctadiene, respectively. After 1 h, about 0.5 μL (or 0.5 mg) of the competing guest was added, and the NMR tube sealed and stored at 298 K until equilibrated.

In CD$_3$CN. In a glovebox, a NMR tube was charged with 0.5–0.7 mL of the 1.0 mM stock solution of $[\mathbf{2}](CF_3SO_3)_8$, respectively, and about 0.5 μL of cyclopentane or 1,5-cyclooctadiene, respectively. After 1 h, about 0.5 μL (or 0.5 mg) of the competing guest was added, and the NMR tube sealed and stored at 298 K until equilibrated.

■ ASSOCIATED CONTENT

Supporting Information

Complete experimental procedures including full characterization, NMR data, ESI mass spectra, and molecular models of host–guest complexes, VT experiments, and crystallographic data. Crystallographic data have also been deposited with the CCDC (file no. 976921). This material is available free of charge via the Internet at http://pubs.acs.org.

■ AUTHOR INFORMATION

Corresponding Author

jrn34@cam.ac.uk

Notes

The authors declare no competing financial interest.

■ ACKNOWLEDGMENTS

We thank the National Crystallography Service at Southampton for collecting X-ray data, I. A. Riddell for the measurement of ESI Mass Spectra, and P. Grice and D. Howe for helpful discussions regarding NMR experiments. This work was supported by the Swiss National Science Foundation (SNSF) (J.L.B.) and the European Research Council (ERC), and M.O. was funded by a JSPS RONPAKU (Ph.D. dissertation) Fellowship.

■ REFERENCES

(1) (a) Wang, Q.-Q.; Day, V. W.; Bowman-James, K. *J. Am. Chem. Soc.* **2013**, *135*, 392–399. (b) Xiao, W.; Hu, C.; Ward, M. D. *Cryst. Growth Des.* **2013**, *13*, 3197–3200. (c) Takezawa, H.; Murase, T.; Fujita, M. *J. Am. Chem. Soc.* **2012**, *134*, 17420–17423.

(2) (a) Kohyama, Y.; Murase, T.; Fujita, M. *Chem. Commun.* **2012**, *48*, 7811–7813. (b) Hastings, C. J.; Backlund, M. P.; Bergman, R. G.; Raymond, K. N. *Angew. Chem., Int. Ed.* **2011**, *50*, 10570–10573. (c) Yamauchi, Y.; Fujita, M. *Chem. Commun.* **2010**, *46*, 5897–5899.

(3) (a) Cram, D. J.; Tanner, M. E.; Thomas, R. *Angew. Chem., Int. Ed. Engl.* **1991**, *30*, 1024–1027. (b) Galán, A.; Gil-Ramírez, G.; Ballester, P. *Org. Lett.* **2013**, *15*, 4976–4979. (c) Hart-Cooper, W. M.; Clary, K. N.; Toste, F. D.; Bergman, R. G.; Raymond, K. N. *J. Am. Chem. Soc.* **2012**, *134*, 17873–17876. (d) Yoshizawa, M.; Kusukawa, T.; Fujita, M.; Yamaguchi, K. *J. Am. Chem. Soc.* **2000**, *122*, 6311–6312.

(4) (a) Zhao, C.; Sun, Q.-F.; Hart-Cooper, W. M.; DiPasquale, A. G.; Toste, F. D.; Bergman, R. G.; Raymond, K. N. *J. Am. Chem. Soc.* **2013**, *135*, 18802–18805. (b) Brown, C. J.; Bergman, R. G.; Raymond, K. N. *J. Am. Chem. Soc.* **2009**, *131*, 17530–17531.

(5) (a) Vetticatt, M. J.; Itin, B.; Evans, G. B.; Schramm, V. L. *Proc. Natl. Acad. Sci. U.S.A.* **2013**, *110*, 15991–15996. (b) Schramm, V. L. *Annu. Rev. Biochem.* **2011**, *80*, 703–732. (c) Mayes, H. B.; Broadbelt, L. J.; Beckham, G. T. *J. Am. Chem. Soc.* **2014**, *136*, 1008–1022. (d) Schramm, V. L. *ACS Chem. Biol.* **2013**, *8*, 71–81.

(6) (a) Mosquera, J.; Zarra, S.; Nitschke, J. R. *Angew. Chem., Int. Ed.* **2014**, *53*, 1556–1559. (b) Rivera, J. M.; Martín, T.; Rebek, J., Jr. *Science* **1998**, *279*, 1021–1023. (c) Schneebeli, S. T.; Frasconi, M.; Liu, Z.; Wu, Y.; Gardner, D. M.; Strutt, N. L.; Cheng, C.; Carmieli, R.; Wasielewski, M. R.; Stoddart, J. F. *Angew. Chem., Int. Ed.* **2013**, *52*,

13100−13104. (d) Taira, T.; Ajami, D.; Rebek, J., Jr. *Chem. Commun.* **2012**, *48*, 8508−8510. (e) Mitra, T.; Jelfs, K. E.; Schmidtmann, M.; Ahmed, A.; Chong, S. Y.; Adams, D. J.; Cooper, A. I. *Nat. Chem.* **2013**, *5*, 276−281. (f) Zhang, G.; Mastalerz, M. *Chem. Soc. Rev.* **2014**, *43*, 1934−1947. (g) Schneider, M. W.; Oppel, I. M.; Griffin, A.; Mastalerz, M. *Angew. Chem., Int. Ed.* **2013**, *52*, 3611−3615. (h) Pochorovski, I.; Ebert, M.-O.; Gisselbrecht, J.-P.; Boudon, C.; Schweizer, W. B.; Diederich, F. *J. Am. Chem. Soc.* **2012**, *134*, 14702−14705. (i) Hua, Y.; Ramabhadran, R. O.; Karty, J. A.; Raghavachari, K.; Flood, A. H. *Chem. Commun.* **2011**, *47*, 5979−5981. (j) Kayahara, E.; Iwamoto, T.; Takaya, H.; Suzuki, T.; Fujitsuka, M.; Majima, T.; Yasuda, N.; Matsuyama, N.; Seki, S.; Yamago, S. *Nat. Commun.* **2013**, *4*, 2695 DOI: 10.1038/ncomms3694.

(7) (a) Ferguson, A.; Squire, M. A.; Siretanu, D.; Mitcov, D.; Mathonière, C.; Clérac, R.; Kruger, P. E. *Chem. Commun.* **2013**, *49*, 1597−1599. (b) Kishi, N.; Li, Z.; Yoza, K.; Akita, M.; Yoshizawa, M. *J. Am. Chem. Soc.* **2011**, *133*, 11438−11441. (c) Liu, T.; Liu, Y.; Xuan, W.; Cui, Y. *Angew. Chem., Int. Ed.* **2010**, *49*, 4121−4124. (d) Tidmarsh, I. S.; Taylor, B. F.; Hardie, M. J.; Russo, L.; Clegg, W.; Ward, M. D. *New J. Chem.* **2009**, *33*, 366−375. (e) Pasquale, S.; Sattin, S.; Escudero-Adán, E. C.; Martínez-Belmonte, M.; de Mendoza, J. *Nat. Commun.* **2012**, *3*, 785 DOI: 10.1038/ncomms1793. (f) Argent, S. P.; Adams, H.; Riis-Johannessen, T.; Jeffery, J. C.; Harding, L. P.; Ward, M. D. *J. Am. Chem. Soc.* **2006**, *128*, 72−73. (g) Cook, T. R.; Zheng, Y.-R.; Stang, P. J. *Chem. Rev.* **2013**, *113*, 734−777. (h) Bilbeisi, R. A.; Clegg, J. K.; Elgrishi, N.; de Hatten, X.; Devillard, M.; Breiner, B.; Mal, P.; Nitschke, J. R. *J. Am. Chem. Soc.* **2012**, *134*, 5110−5119. (i) Sawada, T.; Yoshizawa, M.; Sato, S.; Fujita, M. *Nat. Chem.* **2009**, *1*, 53−56. (j) Han, M.; Engelhard, D. M.; Clever, G. H. *Chem. Soc. Rev.* **2014**, *43*, 1848−1860. (k) Turega, S.; Whitehead, M.; Hall, B. R.; Meijer, A. J. H. M.; Hunter, C. A.; Ward, M. D. *Inorg. Chem.* **2013**, *52*, 1122−1132. (l) Young, N. J.; Hay, B. P. *Chem. Commun.* **2013**, *49*, 1354−1379. (m) Chakrabarty, R.; Mukherjee, P. S.; Stang, P. J. *Chem. Rev.* **2011**, *111*, 6810−6918. (n) Shi, Y.; Sánchez-Molina, I.; Cao, C.; Cook, T. R.; Stang, P. J. *Proc. Natl. Acad. Sci. U.S.A.* **2014**, *111*, 9390−9395.

(8) (a) Moyer, B. A.; Custelcean, R.; Hay, B. P.; Sessler, J. L.; Bowman-James, K.; Day, V. W.; Kang, S.-O. *Inorg. Chem.* **2013**, *52*, 3473−3490. (b) Custelcean, R. *Chem. Soc. Rev.* **2014**, *43*, 1813−1824. (c) Dale, E. J.; Vermeulen, N. A.; Thomas, A. A.; Barnes, J. C.; Juricek, M.; Blackburn, A. K.; Strutt, N. L.; Sarjeant, A. A.; Stern, C. L.; Denmark, S. E.; Stoddart, J. F. *J. Am. Chem. Soc.* **2014**, *136*, 10669−10682. (d) Kishi, N.; Akita, M.; Kamiya, M.; Hayashi, S.; Hsu, H.-F.; Yoshizawa, M. *J. Am. Chem. Soc.* **2013**, *135*, 12976−12979. (e) Gole, B.; Bar, A. K.; Mukherjee, P. S. *Chem.−Eur. J.* **2014**, *20*, 2276−2291. (f) Fang, Y.; Murase, T.; Sato, S.; Fujita, M. *J. Am. Chem. Soc.* **2013**, *135*, 613−615. (g) Freye, S.; Michel, R.; Stalke, D.; Pawliczek, M.; Frauendorf, H.; Clever, G. H. *J. Am. Chem. Soc.* **2013**, *135*, 8476−8479. (h) Custelcean, R.; Bonnesen, P. V.; Duncan, N. C.; Zhang, X.; Watson, L. A.; Van Berkel, G.; Parson, W. B.; Hay, B. P. *J. Am. Chem. Soc.* **2012**, *134*, 8525−8534.

(9) Henkelis, J. J.; Fisher, J.; Warriner, S. L.; Hardie, M. J. *Chem.−Eur. J.* **2014**, *20*, 4117−4125.

(10) (a) Pierro, T.; Gaeta, C.; Neri, P. *Supramol. Chem.* **2010**, *22*, 726−736. (b) Whitehead, M.; Turega, S.; Stephenson, A.; Hunter, C. A.; Ward, M. D. *Chem. Sci.* **2013**, *4*, 2744−2751. (c) Browne, C.; Brenet, S.; Clegg, J. K.; Nitschke, J. R. *Angew. Chem., Int. Ed.* **2013**, *52*, 1944−1948.

(11) Mitra, A.; Panda, D. K.; Corson, L. J.; Saha, S. *Chem. Commun.* **2013**, *49*, 4601−4603.

(12) (a) Sham, K.-C.; Yiu, S.-M.; Kwong, H.-L. *Inorg. Chem.* **2013**, *52*, 5648−5650. (b) Ronson, T. K.; Zarra, S.; Black, S. P.; Nitschke, J. R. *Chem. Commun.* **2013**, *49*, 2476−2490. (c) Zhou, X.-P.; Wu, Y.; Li, D. *J. Am. Chem. Soc.* **2013**, *135*, 16062−16065. (d) Dömer, J.; Slootweg, J. C.; Hupka, F.; Lammertsma, K.; Hahn, F. E. *Angew. Chem., Int. Ed.* **2010**, *49*, 6430−6433. (e) Wu, X.; Xu, N.; Zhu, Z.; Cai, Y.; Zhao, Y.; Wang, D. *Polym. Chem.* **2014**, *5*, 1202−1209. (f) Campbell, V. E.; Guillot, R.; Riviere, E.; Brun, P.-T.; Wernsdorfer, W.; Mallah, T. *Inorg. Chem.* **2013**, *52*, 5194−5200. (g) Bunzen, H.; Nonappa; Kalenius, E.; Hietala, S.; Kolehmainen, E. *Chem.−Eur. J.* **2013**, *19*, 12978−12981. (h) Yi, S.; Brega, V.; Captain, B.; Kaifer, A. E. *Chem. Commun.* **2012**, *48*, 10295−10297.

(13) Coles, S. J.; Gale, P. A. *Chem. Sci.* **2012**, *3*, 683−689.

(14) Kleywegt, G. J.; Jones, T. A. *Acta Crystallogr., Sect. D: Biol. Crystallogr.* **1994**, *50*, 178−185.

(15) Chifotides, H. T.; Dunbar, K. R. *Acc. Chem. Res.* **2013**, *46*, 894−906.

(16) Su, X.; Aprahamian, I. *Chem. Soc. Rev.* **2014**, *43*, 1963−1981.

(17) *Discovery Studio 3.5*; Accelrys Software Inc.: San Diego, CA, 2012.

(18) Mecozzi, S.; Rebek, J., Jr. *Chem.−Eur. J.* **1998**, *4*, 1016−1022.

(19) Turega, S.; Cullen, W.; Whitehead, M.; Hunter, C. A.; Ward, M. D. *J. Am. Chem. Soc.* **2014**, *136*, 8475−8483.

(20) (a) Mugridge, J. S.; Zahl, A.; van Eldik, R.; Bergman, R. G.; Raymond, K. N. *J. Am. Chem. Soc.* **2013**, *135*, 4299−4306. (b) Ruelle, P.; Kesselring, U. W. *J. Pharm. Sci.* **1998**, *87*, 987−997.

(21) Clayden, J. *Nat. Chem.* **2011**, *3*, 842−843.

(22) (a) Zhang, K.-D.; Ajami, D.; Gavette, J. V.; Rebek, J., Jr. *J. Am. Chem. Soc.* **2014**, *136*, 5264−5266. (b) Ajami, D.; Rebek, J., Jr. *Nat. Chem.* **2009**, *1*, 87−90.

(23) Thomson, M. *ArgusLab*; Planaria Software LLC: Seattle WA, 1996.

(24) Chapman, R. G.; Sherman, J. C. *J. Org. Chem.* **2000**, *65*, 513−516.

(25) Biros, S. M.; Bergman, R. G.; Raymond, K. N. *J. Am. Chem. Soc.* **2007**, *129*, 12094−12095.

(26) Albrecht, M.; Burk, S.; Weis, P. *Synthesis* **2008**, *2008*, 2963−2967.

(27) Bolliger, J. L.; Belenguer, A. M.; Nitschke, J. R. *Angew. Chem., Int. Ed.* **2013**, *52*, 7958−7962.